

Mechanisms for slow strengthening in granular materials

W. Losert¹, J.-C. Géminard^{1,2}, S. Nasuno^{1,3}, and J.P. Gollub^{1,4}

¹ *Physics Department, Haverford College, Haverford, PA 19041*

² *Laboratoire de Physique de l'E.N.S. de Lyon, 46 Allée d'Italie, 69364 Lyon Cedex, France*

³ *Department of Electrical Engineering, Kyushu Institute of Technology, Tobata, Kitakyushu 804-8550, Japan*

⁴ *Physics Department, University of Pennsylvania, Philadelphia, PA 19104*

(October 12, 2018)

Several mechanisms cause a granular material to strengthen over time at low applied stress. The strength is determined from the maximum frictional force F_{max} experienced by a shearing plate in contact with wet or dry granular material after the layer has been at rest for a waiting time τ . The layer strength increases roughly logarithmically with τ *only* if a shear stress is applied during the waiting time. The mechanisms of strengthening are investigated by sensitive displacement measurements and by imaging of particle motion in the shear zone. Granular matter can strengthen due to a slow shift in the particle arrangement under shear stress. Humidity also leads to strengthening, but is found not to be its sole cause. In addition to these time dependent effects, the static friction coefficient can also be increased by compaction of the granular material under some circumstances, and by cycling of the applied shear stress.

PACS: 83.70.Fn, 81.40.Pq, 45.70.Cc, 62.40.+i

I. INTRODUCTION

The strength of granular matter is an important macroscopic property. Under many circumstances a layer of granular material at rest can sustain a load, i.e. it behaves like a solid. However, applied shear forces can lead to partial fluidization, a phenomenon that has no direct analog in homogeneous materials [1]. The threshold shear stress σ_{Max} needed to initiate flow also determines when a granular material will lose much of its ability to sustain loads, and is therefore a good measure of strength.

The shear strength of a granular layer is of great interest in geophysical applications, due to the granular composition of earthquake faults. Various studies (described in section II) have shown a gradual strengthening of a granular layer at geophysical pressures, as the time between stress relieving events is increased. Since strengthening of geophysical faults can affect the temporal distribution of earthquakes (see Ref. [11] for references), understanding the underlying mechanisms and developing appropriate models is of practical interest [3].

In previous studies by our group [4–6] the frictional properties of wet and dry sheared granular materials at low pressures were determined in detail by shearing the layer by means of a plate resting upon it. At small applied stresses, high resolution stress and displacement measurements can provide an accurate determination of the instantaneous frictional force experienced by the plate. The static friction coefficient μ_s (the ratio of the threshold static shear stress σ_{Max} to normal stress) was found to be reproducible under given experimental conditions. However, changes in the experimental history influence μ_s . In this article we study the effect of the experimental history on the threshold static shear stress of granular material at low applied normal stress. One central parameter of the experimental history is the waiting time τ for which the layer has been at rest. In addition, the shear stress and humidity during the waiting time are varied; and measurements are made in fluid saturated material. The effects of applied stress reversal are also studied.

In order to determine mechanisms for strengthening, we measure the instantaneous frictional force and the instantaneous vertical dilation of the layer during waiting and during motion. We also image a cross section of the granular layer in some experiments and track the motion of individual grains during waiting and during motion of the plate. Our results indicate that several different mechanisms are needed to account for the observed strengthening. We find that granular matter can strengthen due to a slow shift in the particle arrangement under shear stress. This observation is consistent with a model for granular matter as consisting of a fragile network of stress chains that adjusts to the applied stress [25]. Strengthening is also influenced by humidity, since condensation of liquid bridges

adds an attractive surface tension force between grains [28]. We show clearly that this cannot be the only cause of strengthening by carrying out experiments under water, where liquid bridges cannot be formed. Finally, strengthening may occur by the evolution of individual microcontacts through slow creep [9,10]. Our experiments are not sufficiently sensitive to determine whether creep on length scales of the size of microcontacts actually occurs. However, strengthening of individual contacts alone cannot account for the experimental results. In addition to these slow time-dependent effects, the static friction coefficient can also be increased by compaction of the granular material under some circumstances, and by cycling of the applied shear stress.

Relevant work on friction and work related to proposed strengthening mechanisms are discussed in section II. The experimental results are described in sections III and discussed in section IV.

II. BACKGROUND

A. Strengthening in solid-on-solid friction

In friction between dry solid surfaces (solid-on-solid friction) the static friction coefficient μ_s is determined by the number and strength of microcontacts that support the applied stress (for recent reviews on friction, see Refs. [7,8]). Since the strength of microcontacts changes with time or applied stress, and since their number changes as well through stress-induced creep, μ_s is not a constant, but is influenced by the state of the system. The static friction coefficient - the ratio of the shear force needed to initiate sliding to the normal force - has generally been found to increase approximately logarithmically with the time of (quasi)-stationary contact between materials.

The static strength of a glass-on-glass interface was recently investigated experimentally by Berthoud *et al.* [9,10]. In addition to logarithmic strengthening, the authors find that the rate of increase grows with the temperature of the material. The strengthening rate is twice as high when a shear stress is applied during the waiting time, but strengthening persists without an applied shear stress. This strengthening was found to be a result of an increase in the load bearing area through load-induced creep of individual microcontacts.

B. Strengthening in geophysical experiments

In studies at geophysical pressures (~ 20 MPa) using simulated fault gouge (granular quartz powder) Marone *et al.* [2,11] found logarithmic strengthening of a granular layer with time, if shear stress is applied during the waiting time. On the other hand, when the shear stress is removed, an immediate strengthening of the material is observed followed by a slow weakening with waiting time. Nakatani *et al.* [12] showed that the magnitude of the instantaneous strengthening is proportional to the amount by which the applied shear stress is reduced. These effects are suggested to be a consequence of 'overconsolidation' i.e. rearrangement of particles into a more compact configuration.

C. Rate and state theories

In order to describe the dependence of the frictional force on the state of the system, rate and state theories were developed by Dieterich [13] and Ruina [14], which introduce an additional variable Θ that characterises the system state. In general, several variables might be necessary to describe the state of the system, but the two models focus on the simplest possible case of one state variable determining the system state. In both theories the frictional force is given by

$$\mu = \mu_0 + a \ln \frac{V}{V_0} + b \ln \frac{V_0 \Theta}{D_c} \quad (1)$$

where μ_0 , V_0 , and D_c are characteristic constants of the materials, and V is the instantaneous sliding velocity. In this approach one does not distinguish between static and dynamic cases. The models differ in the differential equation for the state variable Θ . In the Ruina model, for which $d\Theta/dt = -V\Theta/D_c \ln[V/\Theta D_c]$, creep is necessary ($V \neq 0$) to change Θ . On the other hand, time of contact alone increases Θ and thereby μ in the Dieterich model, where

$d\Theta/dt = 1 - V/\Theta D_c$. Different equations have also been proposed by Nielsen, Carlson and Olsen [15] to describe earthquake faults. In their model, Θ changes both with the time of contact and with creep using a characteristic strengthening time τ_c and a characteristic weakening length of contacts l_c ($d\Theta/dt = (1 - \Theta)/\tau_c - \Theta V/l_c$). The friction coefficient is determined by Θ and increases with velocity with a viscous coefficient η ($\mu = \Theta + \eta V$).

While they successfully explain important earthquake characteristics [3], these rate and state models do not describe the instantaneous strengthening when the shear stress is released during a waiting time [11,12].

D. Force transmission in granular media

In solid-on-solid friction, the microcontacts form a two-dimensional disordered array at the interface between the solids. In granular materials, however, simulations indicate that several layers of grains move during the shearing process [16–19]. This is not entirely surprising, given that the interior of the material is not stronger than the surface region, as long as there are no cohesive forces between particles. In order to study granular friction theoretically, one therefore must analyse a three dimensional network of microcontacts. The failure of a subset of those contacts allows motion of the shearing plate. Distinct element method simulations by Morgan *et al.* [19,20] indicate that the grain size distribution and interparticle frictional properties can strongly affect the shear stress necessary for a failure of that contact network and thus granular flow.

Microcontacts can be characterized by the total force and shear force on the contact, and the orientation of the microcontact relative to the total applied stress. Recent experiments have shown that the distribution and orientation of individual particle contacts is highly nonuniform and hysteretic. Shear and normal stresses are transmitted along stress chains, as for example demonstrated in recent simulations by Radjai *et al* [21] and in experiments using birefringent disks by Howell *et al.* [22]. The magnitude of stress between particles follows an exponential probability distribution [22] unless the packing fraction exceeds a critical threshold. The arrangements of stress chains strongly depends on the history of the sample. Small particle rearrangements, e.g. through heating of an individual particle, can alter the stress transmission [23]. Recent experiments by Vanel *et al.* [24] have revealed that the stresses at the bottom of a sandpile can have either a maximum or a local minimum at the center, depending on the preparation procedure. This experiment indicates that even the preferential direction of stress chains may be affected by the history of the sample. One model of stress transmission by Cates *et al.* [25] does not try to develop a stress-strain relations, but instead relates different components of the stress tensor to each other. The granular material is described as a fragile network of stress transmitting contacts. If the direction of the applied stress changes, the network breaks. Simulations by Radjai *et al.* [21] suggest that the network of stress chains can be separated into a strong subnetwork in which most contact surfaces are perpendicular to the direction of total stress, and a weak subnetwork of contacts oriented preferentially perpendicular to it. The weak subnetwork sustains shear stress and breaks through frictional sliding between bead surfaces. The strong subnetwork sustains the normal load, and its contacts change mostly through rolling.

E. Role of dilation

It has been known since Reynolds [26] that shearing a granular material produces dilation, i.e. an expansion of the material in the direction perpendicular to the motion. In wet granular materials, our group found that a granular layer dilates by 10% of one grain diameter while the top layer is translated by one grain diameter [6]; this observation suggests that at most a few layers are involved in the dilation. Computer simulations by Thompson and Grest [17] and Zhang and Campbell [27] have indicated that dilation is prominent in stick-slip motion. A region of about 6-12 grain diameters typically dilates and starts to flow in the simulations at small normal forces. Zhang and Campbell found an approximately linear decrease in particle velocity with depth at high normal forces, and a faster than linear decrease at low normal forces.

Experiments at geophysical pressures by Marone have shown that the granular layer becomes compacted during the waiting time at high normal stresses [11]. Marone notes that compaction increases in proportion to the frictional strength of the material; this indicates a close relation between compaction and strength. The role of dilation therefore should be investigated in connection with measurements of the frictional strength.

F. Role of humidity

Experiments in a rotating cylinder [28] have indicated that strengthening of granular material (indicated by an increased critical angle of repose) might be due to the formation of liquid bridges, which introduce attractive capillary forces between grains. A logarithmic increase of the critical angle of repose of the pile with waiting time was observed. The rate of increase was found to depend strongly on humidity and no strengthening occurred for bead diameters $d > 500\mu\text{m}$ or for vanishing humidity. This behavior is consistent with liquid bridges being the sole cause of strengthening in this study, but angle of repose experiments only look at strengthening in the limit of very small stress, where the role of other strengthening mechanisms might be diminished.

We varied the humidity in some experiments and carried out experiments under water, where liquid bridges cannot form, in order to distinguish this mechanism of strengthening from other possibilities.

G. This work on strengthening in granular materials

Judging from the three dimensional nature of the sheared region, the role of dilation, humidity, and the nonuniform and hysteretic transmission of stress through a granular material, we cannot expect *a priori* that the laws that govern strengthening of solids will hold for granular materials.

In our experiments a small, but non-negligible normal force is applied to the granular material, in contrast to the strengthening studies based on the critical angle of repose. On the other hand, the applied normal force is smaller than the one used in geophysical experiments by a factor of about 10^6 . The threshold stress for plastic deformation of the glass particles is reached for an approximate area for individual microcontacts of the order of 25 nm^2 per particle in our experiments [29]. Creep of individual microcontacts would therefore be at the nm scale, which cannot be resolved with our apparatus. Particle fracture - which occurs in geophysical experiments and yields characteristic grain size distributions - plays no role in our studies. With the ability to image the motion of particles and to measure creep and dilation on the μm scale, our experiments focus on the role of the arrangement of microcontacts (the fabric of the granular material) in determining its shear strength.

III. EXPERIMENTAL RESULTS

A. Apparatus

The experimental setup, shown in Figure 1 has been described previously [4], including the modifications for experiments under water [6]. Our experiments were carried out in a thin 3mm layer of $103 \pm 14\mu\text{m}$ diameter glass beads (Jaygo Inc.) in a $11 \times 18.5\text{cm}$ tray. A transparent acrylic plate ($5.28 \times 8.15\text{cm}$) of weight 26.7 g is placed on top of the granular material. Good contact between plate and layer is assured either by etching grooves or gluing a layer of beads to the plate's lower surface. The plate is pushed across the granular material by a spring that touches only a small steel ball glued to the plate; this allows for vertical motion of the plate. The spring's fulcrum is moved toward the plate at constant speed by a microstep stepper motor. Bending of the spring is measured with a displacement sensor, which indicates the force applied to the plate by the spring with a relative precision of better than 0.1%. The vertical position of the plate is measured with a second displacement sensor having a resolution of $\sim 0.1\mu\text{m}$. As indicated in Figure 1, the granular material and the plate are kept under water in some experiments. The motion of particles is imaged from the side with a fast camera (Kodak Motioncorder SR-500).

B. Particle motion in sheared granular layers

In order to establish how deeply the motion of the top plate penetrates into the granular material, we image the position of glass beads at the side of the cell. A $5.3 \times 18.5\text{cm}$ tray - slightly wider than the plate - was designed with smooth glass sidewalls to allow for optimal visualization. Through direct illumination we obtain small circular bright spots for all beads close to the wall. We track the motion of all particles in the layer closest to the wall from images

taken at 500 frames per second during motion of the plate. (The motion is captured during one slip in the stick-slip regime, which is described in section III C). The changes in bead positions between frames are used to calculate the particle tracks and instantaneous velocities. Since the conditions at the wall are not identical to the inside of a granular material, motion of particles near the side yield only an approximation of particle motion in the interior. However, the observations regarding the depth profile and nonuniformity of motion are unlikely to be qualitatively different for the interior.

One measurement, where ≈ 2000 glass beads are tracked during a short (40ms) slip, is shown in Figure 2. Individual particle velocities and directions of motion are indicated by the direction and length of individual lines. Approximately 5 layers of beads are moving. The particle velocity decreases more strongly with depth than would be the case for a fluid, but qualitatively very similar to simulations [17]. The motion of neighboring particles is not perfectly correlated but differs in direction and velocity. This indicates that the material cannot be described as a solid with a single fracture plane, but that most individual particle contacts are broken up. Slip of the plate therefore involves the breakup of most particle contacts within about 5 layers close to the plate: this process is quite different from the breakup of a 2D array of contacts that occurs when a solid starts sliding on another solid. A more detailed study of particle motion is in progress and will be reported elsewhere [33].

C. Strengthening in dry granular materials

In dry granular materials stick-slip motion with long sticking times and short, fast slips is the prevalent behavior at constant motor speed in our experiments. The strength of the material was therefore measured from the spring displacement, i.e. the maximum spring displacement prior to a slip. In the steady state, the slip reproducibly starts at the same spring displacement, but the first slip after the motor is started can be different. In the first set of experiments to be considered, the motor is stopped during stick-slip motion and restarted after a waiting time τ . The applied stress during waiting varies by roughly 30% (depending on how long after a slip event the motor is stopped). Figure 3 shows the spring displacement vs time, with the motor started at $t = 1.19$ s after a waiting time $\tau = 22$ s (dotted line), $\tau = 1130$ s (dashed line), or $\tau = 26,400$ s (solid line). The total spring displacement before the first slip increases with waiting time, but after at most two slips a steady stick-slip motion is reached with the same maximum spring displacement for all waiting times (the curves are offset by $150\mu\text{m}$).

In some experiments no shear stress was applied during the waiting time by moving the motor backward prior to waiting. The spring displacement when the motor started with a completely unbent spring at $t = 8.2$ s after a waiting time of 37,213 s is shown in figure 4. After several slips the motor direction is reversed at $t = 50$ s. In this case, the stress just before the first slip is not enhanced. At low normal stress in the stick-slip regime, the strength of dry granular material therefore only increases with waiting time if a shear stress is applied during the waiting time.

The ratio of the maximum spring displacement prior to the first slip F_{max} to the average maximum spring displacement F_{norm} of all except the first two slips indicates the relative strengthening of the material with waiting time. This ratio is shown in figure 5 for the stressed case. The waiting time strengthening under shear stress appears to be faster than logarithmic when the full range of waiting times τ is included. On shorter timescales the material becomes roughly 2% stronger (compared to continuous stick-slip motion) per decade increase in τ . On longer timescales $\tau > 1000$ s the strengthening is roughly 10% per decade with a characteristic initiation time τ_0 (the time before which little strengthening occurs based on an extrapolation of the approximately logarithmic increase) of roughly 600 ± 300 s.

D. Role of Dilation

The vertical position $h(t)$ of the plate indicates the dilation or compaction of the granular material. Due to small deviations from perfect flatness of the target plate for the vertical displacement sensor and slow fluctuations in the sensor readout due to small variations in temperature, the absolute dilation cannot be computed to better than $1\mu\text{m}$ over long times or over horizontal plate movements long compared to the particle diameter.

Figure 6 shows the vertical plate position after a waiting time under shear stress for the experiments described in Figure 3. After the motor is started, a gradual dilation of the granular material during the sticking time takes place, followed by rapid dilation as the slip starts and compaction immediately following the slip. The first slip after a long waiting time (solid line) is followed by especially strong compaction.

The vertical dilation *without* applied shear stress during waiting is shown in Figure 7, which corresponds to the spring displacement data of Figure 4. As the plate starts to move, the layer gradually dilates. The gradual dilation does not influence the maximum frictional force, which is comparable for all slips as shown in Figure 4. As soon as the shear stress is released at $t > 60$ s, the layer compacts almost instantaneously.

E. Strengthening under water

Since the formation of liquid bridges between particles could be the cause for the observed strengthening of granular material, as described in [28], a second set of experiments was carried out under water, where liquid bridges are absent. Continuous sliding is prevalent under water because the fluid lubricates the contacts. Figure 8 shows the typical behavior of the spring displacement $d(t)$ (Fig. 8a) and of the vertical position $h(t)$ (Fig. 8b) as functions of time t in two different cases: (1) The horizontal stress is released before the experiment; (2) The horizontal stress is continuously applied. In both cases the spring displacement during the transient (which is proportional to the frictional force at the small accelerations considered here) is larger than the frictional force during steady sliding. The force reaches a maximum F_{max} at the maximum dilation rate. At later times the material continues to dilate and approaches a steady state dilation, while the frictional force decreases toward a steady sliding frictional force. In case (2), the layer is initially less packed and the total dilation Δh observed during the experiment is smaller.

As observed for the dry granular material, we find that the maximum frictional force F_{max} depends on the resting time τ , and on the horizontal stress applied during this interval, as shown in Figure 9. The experimental procedure is as follows: The plate is initially pushed at constant velocity ($28.17\mu\text{m/s}$) until the steady state regime is reached with a dynamic friction force F_d . Then, the motion of the translator is suddenly stopped and the plate stops at a well-defined horizontal applied stress ($F = 3.2 \cdot 10^{-2}N \simeq F_d$) [30]. The translator motion is started again after a delay τ . As for dry granular materials, we find that the maximum value of the frictional force F_{max} depends on the waiting-time τ : The maximum frictional force increases by roughly 10% of F_d for each order of magnitude increase in waiting time with a characteristic initiation time $\tau_0 = 0.6 \pm 0.2$ s, a factor of $\sim 10^3$ faster than for a dry granular material. The maximum frictional force F_{max} increases by about 40% in 10 hours. On the other hand, if no horizontal stress is applied during the waiting-time τ (the spring is pulled back), no increase of the maximum frictional force is measured. For short waiting times F_{max} is found to be larger when no stress is applied; this result is in agreement with the fact that the maximum frictional force increases with the total dilation of the layer Δh in the continuous sliding case for a wet granular material [6]. The two curves for strengthening with and without applied shear stress intersect for $\tau \simeq 10^4$ s. For longer waiting times F_{max} becomes larger for waiting under an applied shear stress while the dilation following the waiting (Δh) remains larger when no stress is applied.

A careful study of the behavior of the vertical position of the plate h as a function of its horizontal position x shown in Figure 10 indicates that h reaches a maximum during the transient regime when a horizontal stress is applied during the waiting time. The distance over which the vertical position of the plate reaches its maximum is about one particle radius R , comparable to the distance over which the system reaches the steady state regime in experiments starting without applied shear stress [6]. However, after a waiting time under stress, the vertical position of the plate decreases for a sliding distance of a few particle diameters. The frictional force reaches its asymptotic value over the distance R , and appears not to be affected by this decrease of the vertical position of the plate.

Creep during the waiting time can be directly observed. If the plate is kept under a shear stress comparable to the steady sliding value, it creeps slowly ($dx/dt \simeq 1\mu\text{m/h}$) and goes up (Fig.11). Such strong creep has not been observed in dry granular materials. The vertical velocity dh/dt of the plate is of the same order of magnitude as the horizontal velocity dx/dt . Moreover, the whole vertical displacement of the plate δh after 7 hours is about $20\mu\text{m}$, much larger than any vertical displacement of the plate observed in the dynamical regime.

IV. DISCUSSION AND CONCLUSION

The main results of this investigation of the shear strength of a granular material at low normal forces are as follows:

- (a) The strength of a granular material increases roughly logarithmically with the time of stationary contact τ (waiting time) in both dry material (Fig. 5) and wet material (Fig. 9), if a shear stress is applied during the waiting time. The characteristic initiation time τ_0 is roughly three orders of magnitude smaller for wet granular material.

(b) In both dry and wet granular matter, the strength does not increase with τ if no shear stress is applied during the waiting time (Figs. 4 and 9).

(c) In both the dry and the wet granular material, the layer compacts immediately, when the shear stress is released. This compaction leads to an instantaneous increase in the strength of the wet granular material, but not in the dry case (Figs. 4 and 9).

(d) Particle tracking reveals that in a region of approximately 5 particle layers below the sheared surface, particles move and lose contact with each other during stick-slip motion (Fig. 2). The particle velocities within this fluidized region decrease faster than linearly.

(e) Dilation or compaction often influences the strength of the material. However, gradual slight dilation in a dry material (Fig. 7) and gradual slight compaction in a wet material (Fig. 10) do not necessarily influence the frictional forces.

In order to understand these results we need to go back to the main question: What are the microscopic mechanisms for strengthening? In the following paragraphs we look at individual mechanisms and the experimental results that support them or show their limitations.

The gradual strengthening of individual microcontacts through creep on the level of microcontacts has been found in other work to lead to strengthening in solid-on-solid friction. The microcontact size is determined by the yield stress of the material. Unless the contact area is flat, the material deforms until the microcontact is just large enough to support the stress. Strengthening of microcontacts should therefore be present for granular materials with nm scale contact areas just as it is for solid-on-solid friction.

Another mechanism that can strengthen microcontacts is an attractive surface force, created by gradually developing liquid bridges between particles at rest. This mechanism accounts for the observed increase in strengthening at higher humidity, but can not explain why strengthening also occurs for a granular layer under water. Other mechanisms for strengthening must therefore be present.

No strengthening is observed in the absence of an applied shear stress even though the absence of applied shear stress only decreases the total stress on microcontacts by 10 – 20%. In addition, the observed creep distance under water (Fig. 11) is several orders of magnitude larger than the characteristic microcontact length; this suggests that microcontacts break rather than strengthen during the time at rest. Microcontact strength can therefore not account for strengthening under water or the lack of strengthening in the absence of an applied shear stress in both dry and wet material.

The large creep under water suggests that grains rearrange more easily in wet than in dry granular matter. One possible explanation is that water lubricates individual contacts between grains, which allows grains to slip past each other with significantly smaller frictional force. Lubrication is also evident in the reduced friction coefficient of a wet granular material [6]. Even though large creep decreases the contact time of microcontacts, strengthening occurs at the same rate, and with a much smaller characteristic initiation time τ_0 in wet granular matter. This indicates that rearrangements in the network of contacts contribute significantly to strengthening. The rigidity of the network of contacts can influence the frictional strength of the material, since direct observations indicate that a three dimensional network of contacts is broken (and a fluidized region of several layers close to the sheared surface forms) when sliding starts.

The observation of strengthening solely under shear stress differs from results in solid-on-solid friction, but is similar to results at geophysical pressures [2,11]. It implies that the contact network changes in response to an applied shear stress regardless of how the contacts themselves evolve. This is consistent with the description of a granular material as a fragile network that breaks if the direction of the applied stress changes. Recent experiments in a Couette cell, which will be reported in detail elsewhere [34], support the conclusion that the direction of the applied stress matters. In the Couette cell a clockwise shear stress that is less than the slip threshold is first applied for a waiting time τ . If the granular material is subsequently sheared clockwise, a roughly logarithmic increase in the strength with τ is observed, as for the flat layer studied in this paper. On the other hand, if the subsequent shear is counterclockwise, no strengthening is observed.

The density of the granular material is a rough indicator of the density of the contact network, as more grains tend to touch each other in denser configurations. However, compaction and dilation are not always correlated with frictional strength in our experiments, possibly because we are limited to measuring the mean density, not the local density of the surface region, where the network of microcontacts fails. The possibility that the orientation of microcontacts could be as important for the strength of the material as the density of contacts should also be explored further.

When the shear stress is completely released, a significant density change occurs. This suggests that the granular material under normal stress can only compact if the existing contact network breaks - which in our case happens when the shear stress is removed. Recent experiments in a Couette cell [34], show that changing the direction of shear stress can be used to strengthen the granular material rapidly. The inner cylinder of the Couette cell is connected to a motor through a soft spring, which allows for variations in the applied shear force at forces below the frictional strength of the granular material. When the direction of the applied shear stress is reversed periodically at stresses below that necessary to initiate sliding, the strength of the material can be increased rapidly in proportion to the number of direction reversals.

In conclusion, strengthening in these experiments can be explained by two fundamentally different phenomena. One is a strengthening of individual microcontacts due to time of contact or slow creep - or due to the formation of liquid bridges. The other fundamental strengthening mechanism is related to the spatial arrangement of beads and hence the arrangement and orientation of microcontacts. The strength of the contact network (sometimes called the fabric of the granular material) can be related to the compaction of the granular material, but our experiments indicate that compaction is not the only determinant of the strength of the network.

Strengthening due to rearrangements alone can also be related to a wide range of other systems that can jam, such as molecules in a glass. It has recently been suggested [31,32] that some aspects of the jamming behavior, or the 'unjammings' which we study, might have a common theoretical description, so a good understanding of the strengthening might eventually be useful for a description of the properties of these other systems as well.

V. ACKNOWLEDGMENTS

This work was supported by the U.S. National Science Foundation under Grant DMR-9704301. J.-C. G. thanks the Centre National de la Recherche Scientifique (France) for supporting the research of its members carried out in foreign laboratories. The optical measurements were carried out by P. Ingebretson. We appreciate helpful discussions with C. Scholz and C. Marone.

-
- [1] For a review of some unique properties of granular materials see: H.M. Jaeger, S.R. Nagel, and R.P. Behringer, *Rev. Mod. Phys.* **68**, 1259 (1996).
 - [2] S.L.Karner, and C. Marone, *Geophys. Res. Lett.* **25**, 4561 (1998).
 - [3] C. Scholz, *Nature* **391**, 37 (1998).
 - [4] S. Nasuno, A. Kudrolli, A. Bak, and J. P. Gollub, *Phys. Rev. E* **58**, 2161 (1998).
 - [5] S. Nasuno, A. Kudrolli, and J. P. Gollub, *Phys. Rev. Lett.* **79**, 949 (1997).
 - [6] J.C. Géminard, W. Losert and J. P. Gollub, *Phys. Rev. E* **59**, 5881 (1999).
 - [7] G. Hähner and N. Spencer, *Phys. Today* **51**, 23 (1998).
 - [8] J. Krim, *MRS Bulletin* **23**, 20 (1998).
 - [9] P. Berthoud, T. Baumberger, C.G'Sell and J.-M. Hiver, *Phys. Rev. B* **59**, 14313 (1999).
 - [10] T. Baumberger, P. Berthoud, and C. Caroli, *Phys. Rev. B* **60**, 3928 (1999).
 - [11] C. Marone, *Ann. Rev. Earth Plan. Sci.* **26**, 643 (1998).
 - [12] M. Nakatani, *J. Geophys. Res.* **103**, 27239 (1998).
 - [13] J.H. Dieterich, *J. Geophys. Res.* **84**, 2161 (1979).
 - [14] A. Ruina, *J. Geophys. Res.* **88**, 10359 (1983).
 - [15] S.B. Nielsen, J.M. Carlson, and K.B. Olsen, submitted to *J. Geophys. Res.* (1999).
 - [16] D.M. Hanes, and D.L. Inman, *J. Fluid Mech.* **150**, 357 (1985).
 - [17] P.A. Thompson, and G.S. Grest, *Phys. Rev. Lett.* **67**, 1751 (1991).
 - [18] E. Aharonov, and D. Sparks, preprint, cond-mat/9812204.
 - [19] J.K. Morgan, and M.S. Boettcher *J. Geophys. Res.* **104** 2703 (1999).
 - [20] J.K. Morgan, *J. Geophys. Res.* **104** 2721 (1999).
 - [21] F. Radjai, D.E. Wolf, M. Jean, and J.-J. Moreau, *Phys. Rev. Lett.* **80**, 61 (1998).
 - [22] D. Howell, R.P. Behringer, and C. Veje, *Phys. Rev. Lett.* **82**, 5241 (1999).
 - [23] C.H. Liu and S.R. Nagel, *J. Phys* **6**, A433 (1994).
 - [24] L. Vanel, D. Howell, D. Clark, R.P. Behringer, and E. Clément, preprint, cond-mat/9906321.

- [25] M.E. Cates, J.P. Wittmer, J.-P. Bouchaud, and P. Claudin, Phys. Rev. Lett. **81**, 1841 (1998).
- [26] O. Reynolds, Philos. Mag **20**, 469 (1885).
- [27] Y. Zhang and C.S. Campbell, J. Fluid. Mech. **237**, 541 (1992).
- [28] L. Bocquet, E. Charlaix, S. Ciliberto, and J. Crassous, Nature **396**, 735 (1998).
- [29] The contact area is calculated in the approximation that all particles in a layer sustain a roughly equal load.
- [30] At the low speeds of our experiments, the plate does not move much after the motor has been stopped. The shear force during waiting is therefore approximately equal F_d .
- [31] A.J. Liu and S.R. Nagel, Nature **396**, 21 (1998).
- [32] S.F. Edwards, and D.V. Grinev, preprint, cond-mat/9905114.
- [33] W. Losert, P. Ingebretson, and J.P. Gollub, in preparation.
- [34] W. Losert, and J.P. Gollub, in preparation.
- [35] C. Marone, Nature **391**, 69 (1998).

FIG. 1. Schematic diagram of the experimental setup for studying shear in a granular layer with sensitive measurement of horizontal and vertical positions under water and in air.

FIG. 2. Motion of ≈ 2000 particles during a short (40ms) slip. Particles in approximately 5 layers are moving, but the particle speed decreases strongly with depth. (1pixel $\simeq 30\mu\text{m}$).

FIG. 3. Spring displacement vs time at $v = 28.7\mu\text{m/s}$, $k = 189.5\text{N/m}$. The motor is stopped during stick-slip motion and restarted at $t = 1.19\text{s}$ after a waiting time of 22 s (dotted line), 1130 s (dashed line, offset by $150\mu\text{m}$), or 26400 s (solid line, offset by $300\mu\text{m}$). The maximum spring displacement prior to the first slip increases with waiting time. This indicates an increase in the friction coefficient with the waiting time, when the layer is continuously held under stress.

FIG. 4. Spring displacement vs time without initial applied stress ($v = 28.7\mu\text{m/s}$, $k = 189.5\text{N/m}$). The motor started with a completely unbent spring at $t = 8.2\text{ s}$ after a waiting time of 37213 s (solid line). The motor is reversed at $t = 50\text{ s}$. The maximum spring displacement does not change with waiting time.

FIG. 5. Strengthening: Ratio of maximum static friction force F_{max} after a waiting time compared to the maximum static friction force F_{norm} during continuous stick-slip motion at $v = 28.7\mu\text{m/s}$, $k = 189.5\text{N/m}$. The strength increases roughly logarithmically with waiting time for longer times. Each point is an average over several runs.

FIG. 6. Dilation during stick-slip motion (dry). Vertical plate displacement vs time at $v = 28.7\mu\text{m/s}$, $k = 189.5\text{N/m}$. The motor is stopped during stick-slip motion and restarted at $t = 1.19\text{s}$ after a waiting time of 22 s (dotted line), 1130 s (dashed line), or 26400 s (solid line). The compaction following the first slip increases with waiting time; this indicates that dilation occurred during the waiting time.

FIG. 7. Vertical displacement vs time (solid line) and spring displacement (dotted line) for the data of Figure 4 ($v = 28.7\mu\text{m/s}$, $k = 189.5\text{N/m}$). The motor started with a completely unbent spring at $t = 8.2\text{ s}$ after a waiting time of 37213 s. The material dilates when motion starts. The reduction of the applied stress is accompanied by compaction.

FIG. 8. (Wet friction) Behavior (a) of the spring displacement $d(t)$ and (b) of the vertical position $h(t)$ as functions of time t in two different cases: (1) The horizontal stress is released before the experiment; (2) The horizontal stress is continuously applied. In the second case, the layer is initially less packed because of the applied shear stress; as a consequence, the total dilation Δh observed during the experiment is less ($k = 189.5\text{ N/m}$, $M = 14.5\text{ g}$, $V = 28.17\mu\text{m/s}$) (from Ref.[6]).

FIG. 9. (Wet friction) Maximum frictional force F_{max} as a function of the waiting time τ ($k = 189.5\text{N/m}$, $M = 14.5\text{g}$, $V = 28.17\mu\text{m/s}$). Empty circles: no horizontal stress is applied during the waiting time τ . Filled circles: the plate is submitted to a horizontal stress ($F \simeq F_d$) during the waiting-time τ .

FIG. 10. (Wet friction) Vertical position of the plate h as a function of its horizontal position x during a transient. The vertical position overshoots when the plate was subjected to a horizontal stress during the waiting time τ ($k = 189.5\text{N/m}$, $M = 14.5\text{g}$, $V = 28.17\mu\text{m/s}$, $\tau = 26000\text{s}$).

FIG. 11. (Wet friction) Horizontal and vertical positions of the plate x and h as functions of time t when the system is submitted to a static horizontal applied stress $F \simeq F_d$. Creep of about $1\mu\text{m/h}$ is clearly evident ($k = 189.5\text{N/m}$, $M = 14.5\text{g}$).

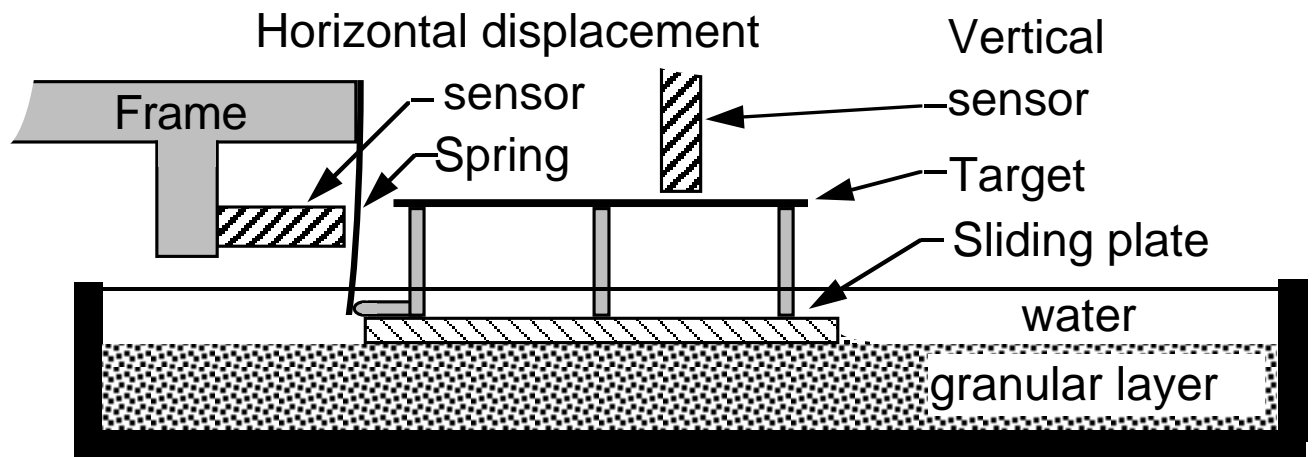


FIG. 1. Schematic diagram of the experimental setup for studying shear in a granular layer with sensitive measurement of horizontal and vertical positions under water and in air.

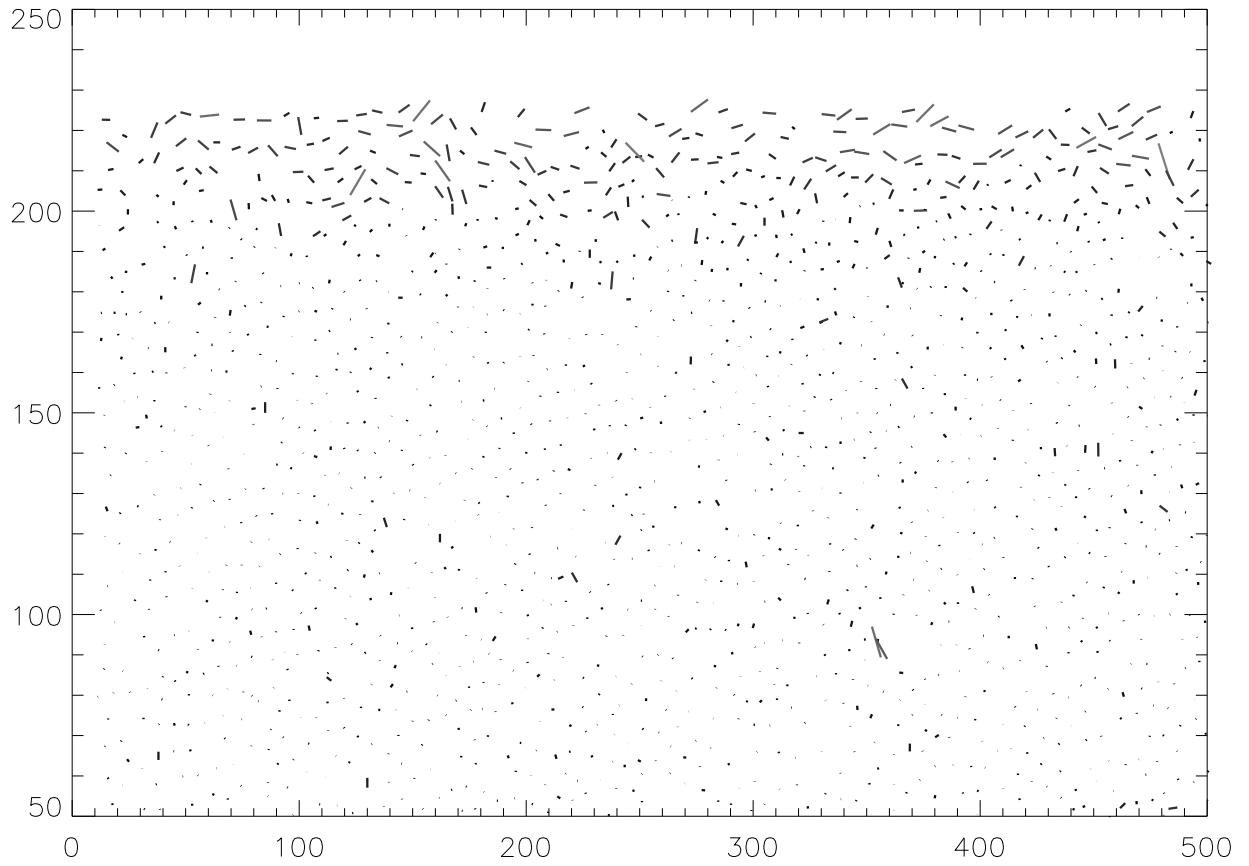


FIG. 2. Motion of ≈ 2000 particles during a short (40ms) slip. Particles in approximately 5 layers are moving, but the particle speed decreases strongly with depth. (1pixel $\simeq 30\mu\text{m}$).

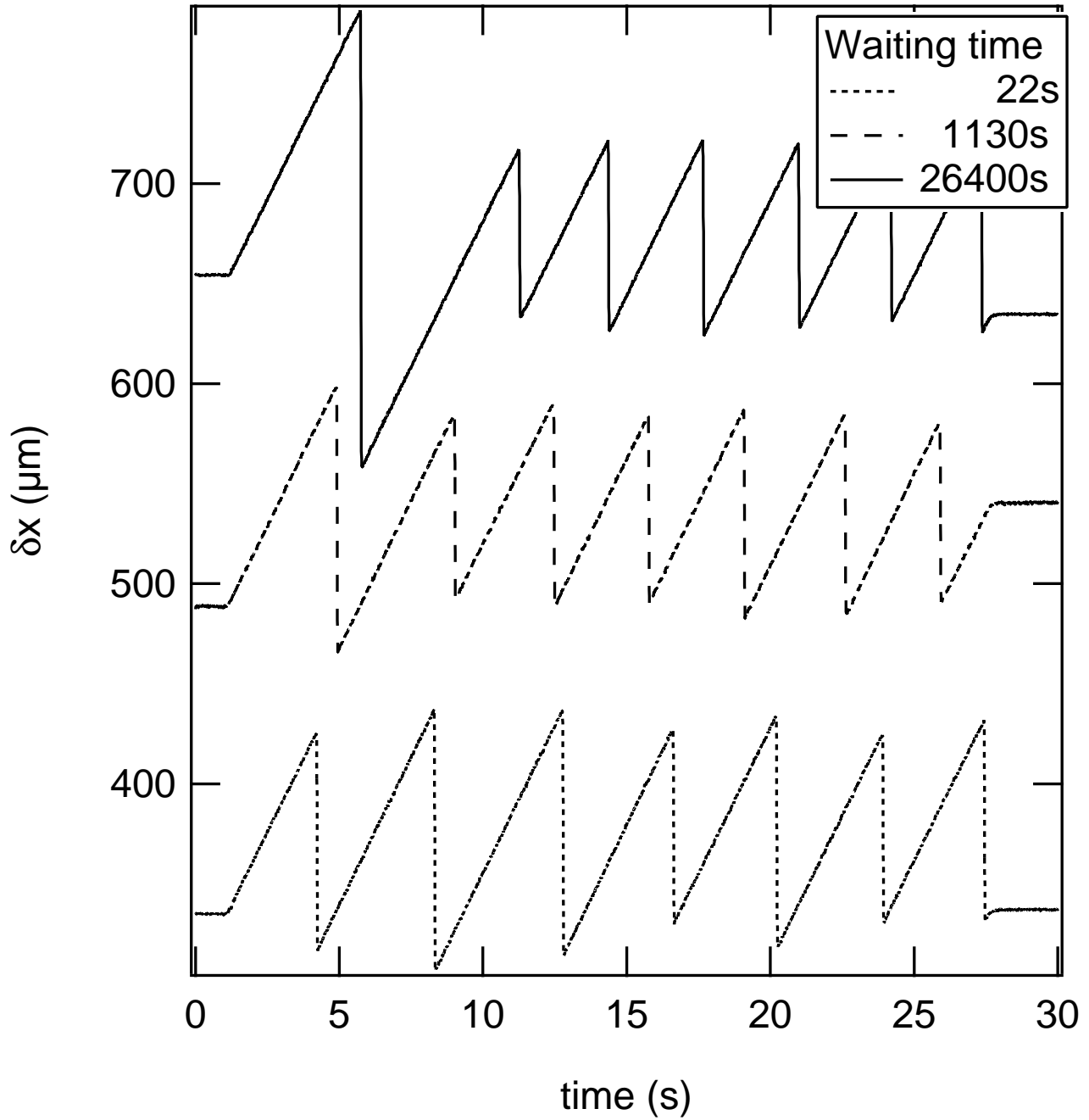


FIG. 3. Spring displacement vs time at $v = 28.7\mu\text{m/s}$, $k = 189.5\text{N/m}$. The motor is stopped during stick-slip motion and restarted at $t = 1.19\text{s}$ after a waiting time of 22 s (dotted line), 1130 s (dashed line, offset by $150\mu\text{m}$), or 26400 s (solid line, offset by $300\mu\text{m}$). The maximum spring displacement prior to the first slip increases with waiting time. This indicates an increase in the friction coefficient with the waiting time, when the layer is continuously held under stress.

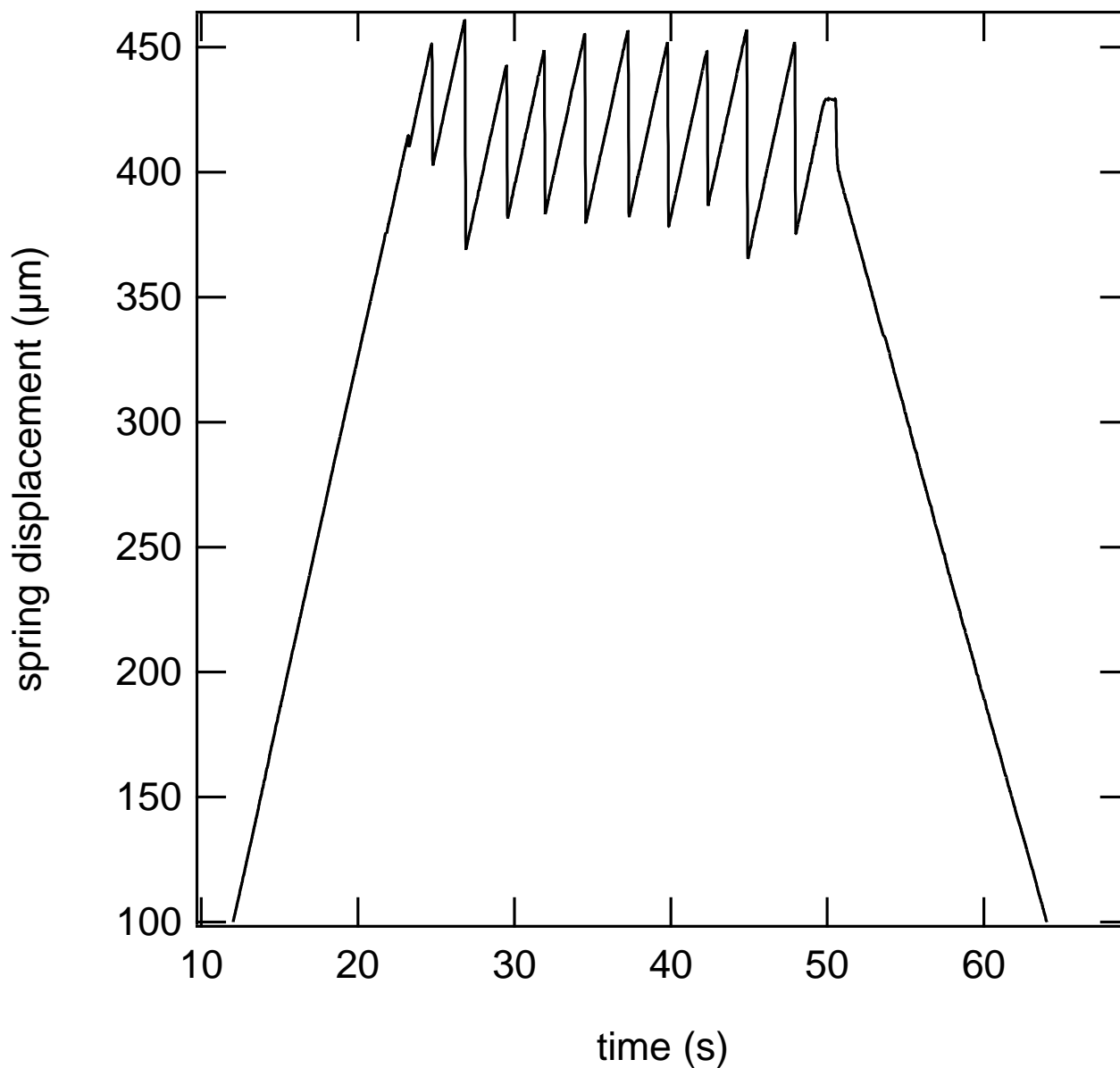


FIG. 4. Spring displacement vs time without initial applied stress ($v = 28.7\mu\text{m/s}$, $k = 189.5\text{N/m}$). The motor started with a completely unbent spring at $t = 8.2$ s after a waiting time of 37213 s (solid line). The motor is reversed at $t = 50$ s. The maximum spring displacement does not change with waiting time.

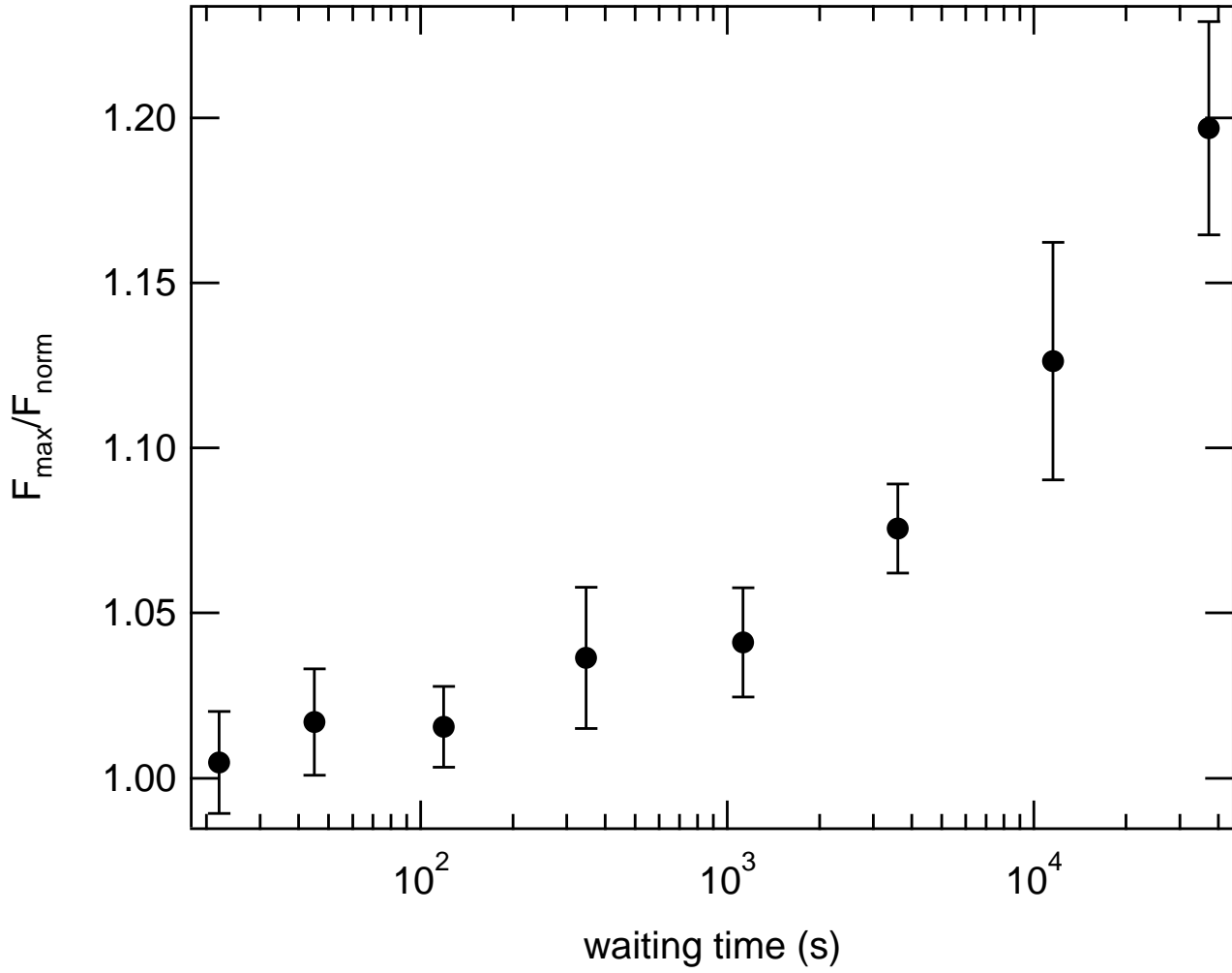


FIG. 5. Strengthening: Ratio of maximum static friction force F_{\max} after a waiting time compared to the maximum static friction force F_{norm} during continuous stick-slip motion at $v = 28.7\mu\text{m/s}$, $k = 189.5\text{N/m}$. The strength increases roughly logarithmically with waiting time for longer times. Each point is an average over several runs.

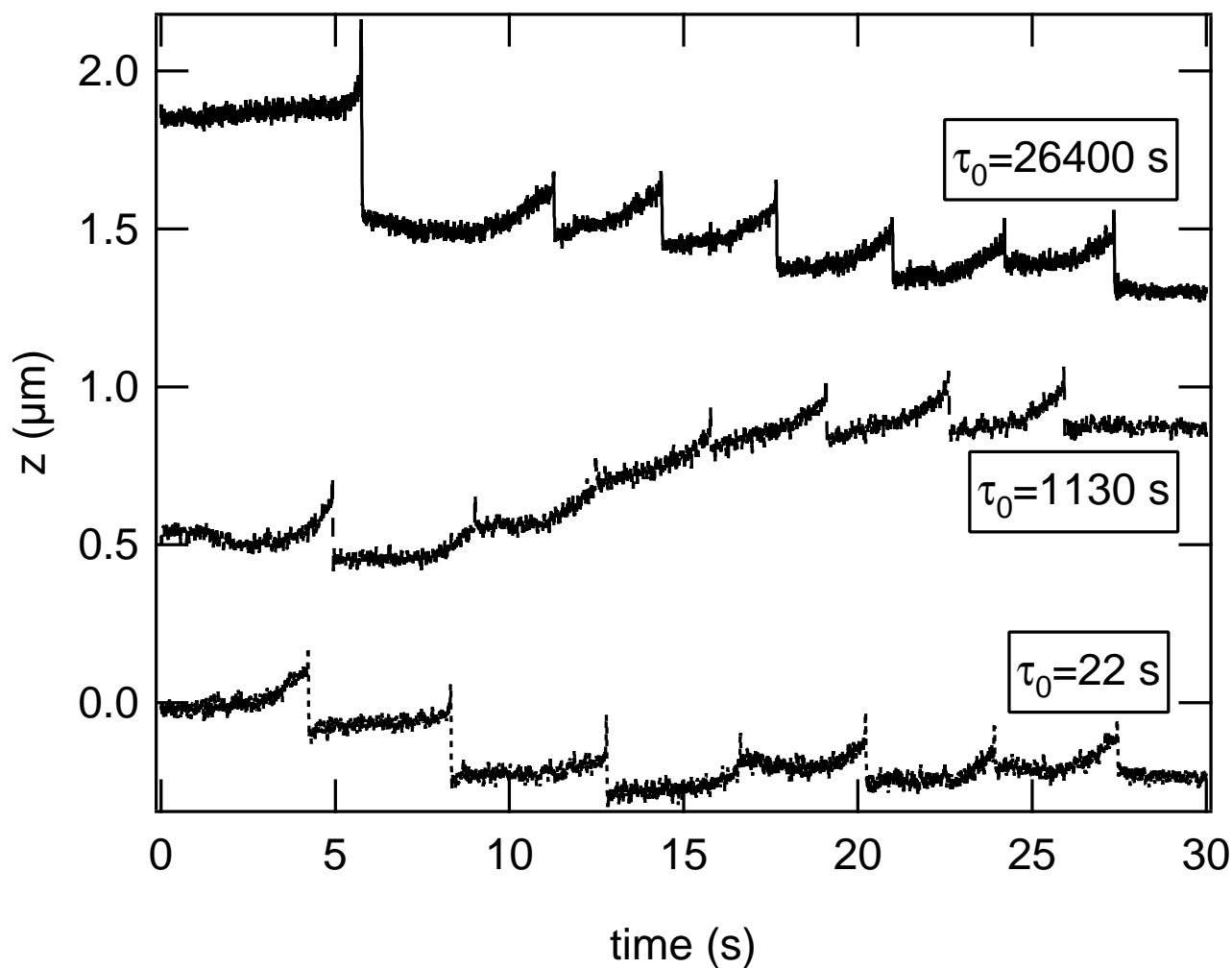


FIG. 6. Dilation during stick-slip motion (dry). Vertical plate displacement vs time at $v = 28.7\mu\text{m/s}$, $k = 189.5\text{N/m}$. The motor is stopped during stick-slip motion and restarted at $t = 1.19\text{s}$ after a waiting time of 22 s (dotted line), 1130 s (dashed line), or 26400 s (solid line). The compaction following the first slip increases with waiting time; this indicates that dilation occurred during the waiting time.

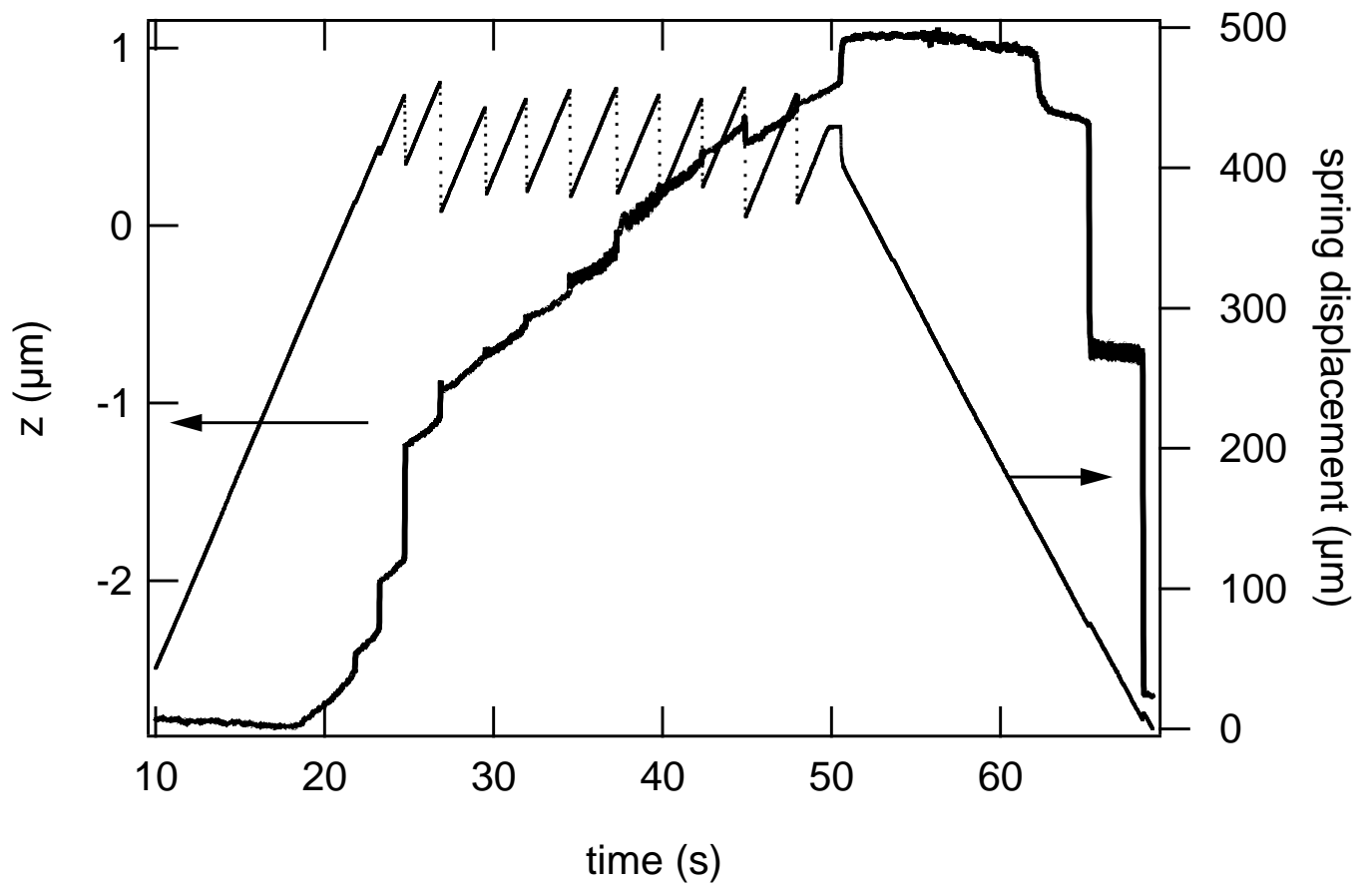


FIG. 7. Vertical displacement vs time (solid line) and spring displacement (dotted line) for the data of Figure 4 ($v = 28.7\mu\text{m/s}$, $k = 189.5\text{N/m}$). The motor started with a completely unbent spring at $t = 8.2$ s after a waiting time of 37213 s. The material dilates when motion starts. The reduction of the applied stress is accompanied by compaction.

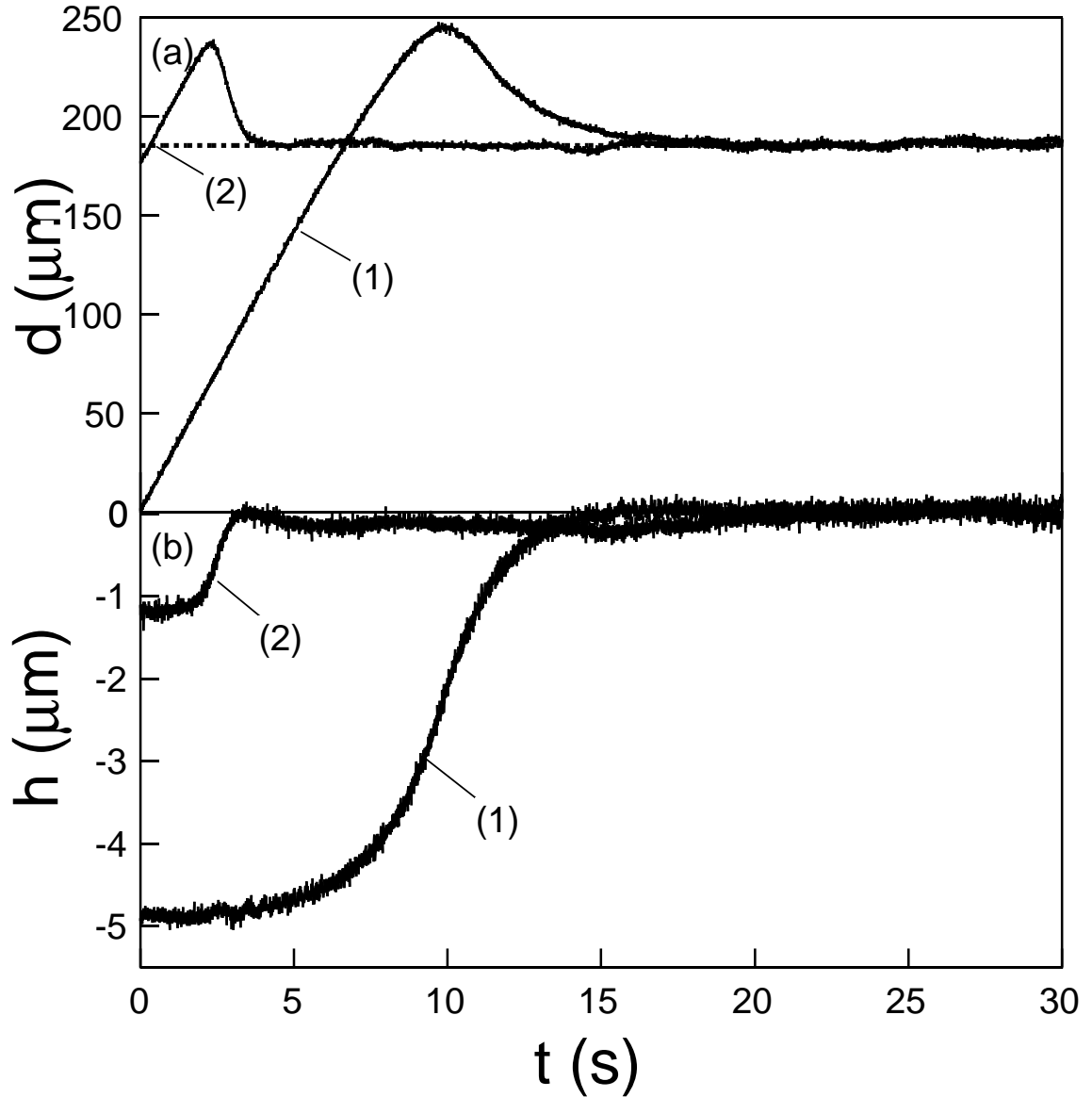


FIG. 8. (Wet friction) Behavior (a) of the spring displacement $d(t)$ and (b) of the vertical position $h(t)$ as functions of time t in two different cases: (1) The horizontal stress is released before the experiment; (2) The horizontal stress is continuously applied. In the second case, the layer is initially less packed because of the applied shear stress; as a consequence, the total dilation Δh observed during the experiment is less ($k = 189.5$ N/m, $M = 14.5$ g, $V = 28.17$ $\mu\text{m/s}$) (from Ref.[6]).

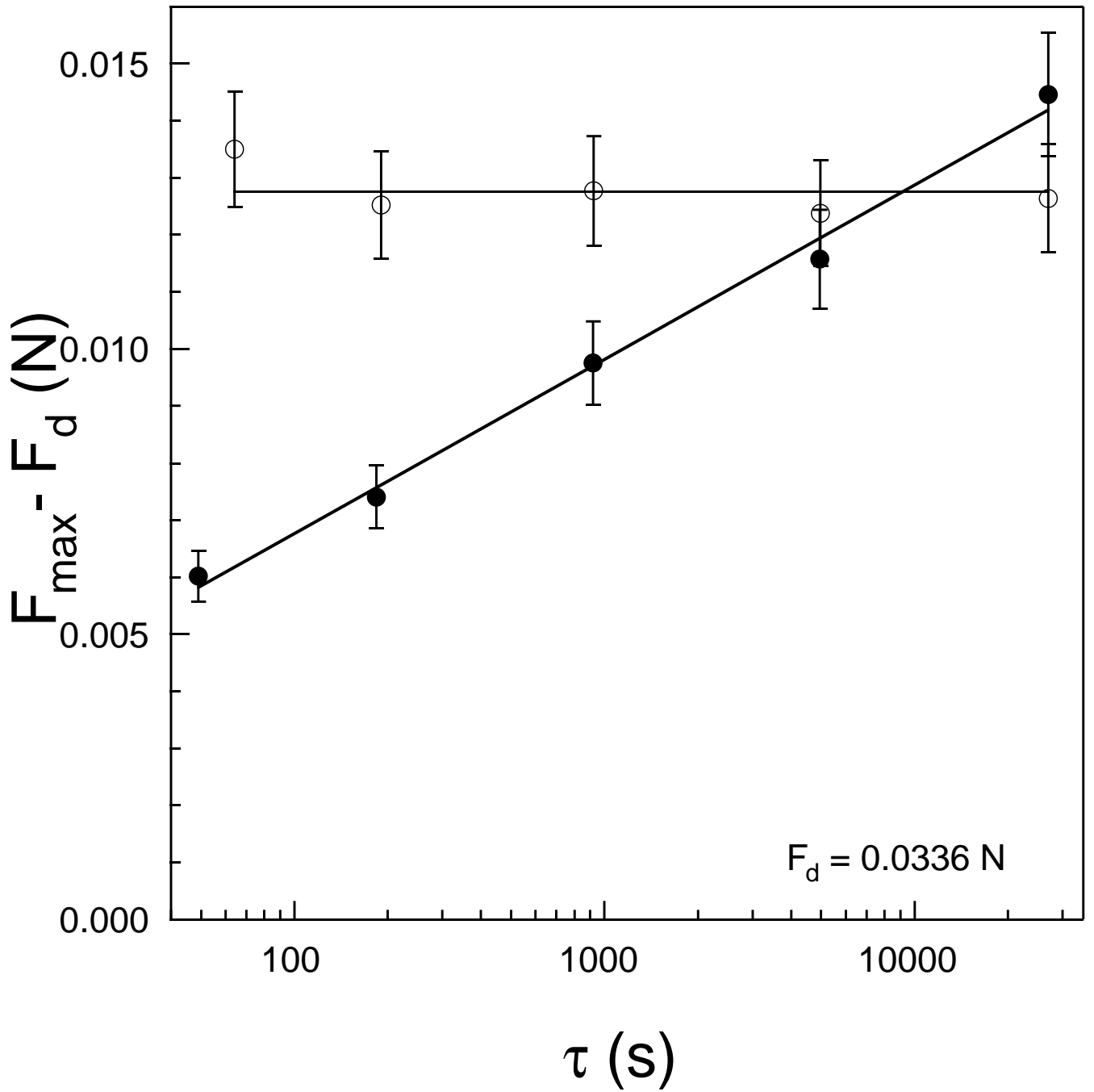


FIG. 9. (Wet friction) Maximum frictional force F_{max} as a function of the waiting time τ ($k = 189.5\text{N/m}$, $M = 14.5\text{g}$, $V = 28.17\mu\text{m/s}$). Empty circles: no horizontal stress is applied during the waiting time τ . Filled circles: the plate is submitted to a horizontal stress ($F \simeq F_d$) during the waiting-time τ .

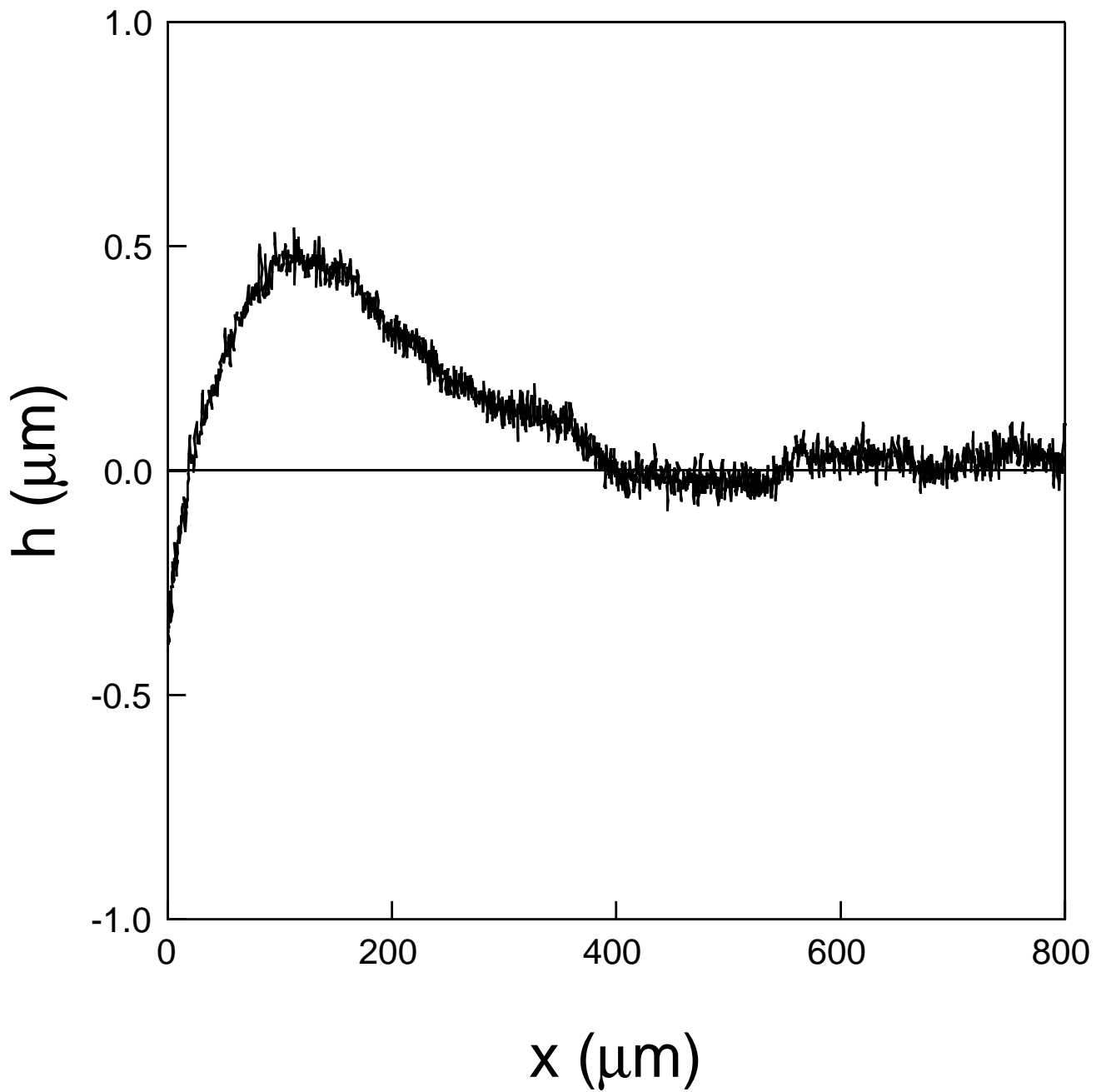


FIG. 10. (Wet friction) Vertical position of the plate h as a function of its horizontal position x during a transient. The vertical position overshoots when the plate was subjected to a horizontal stress during the waiting time τ ($k = 189.5\text{N/m}$, $M = 14.5\text{g}$, $V = 28.17\mu\text{m/s}$, $\tau = 26000\text{s}$).

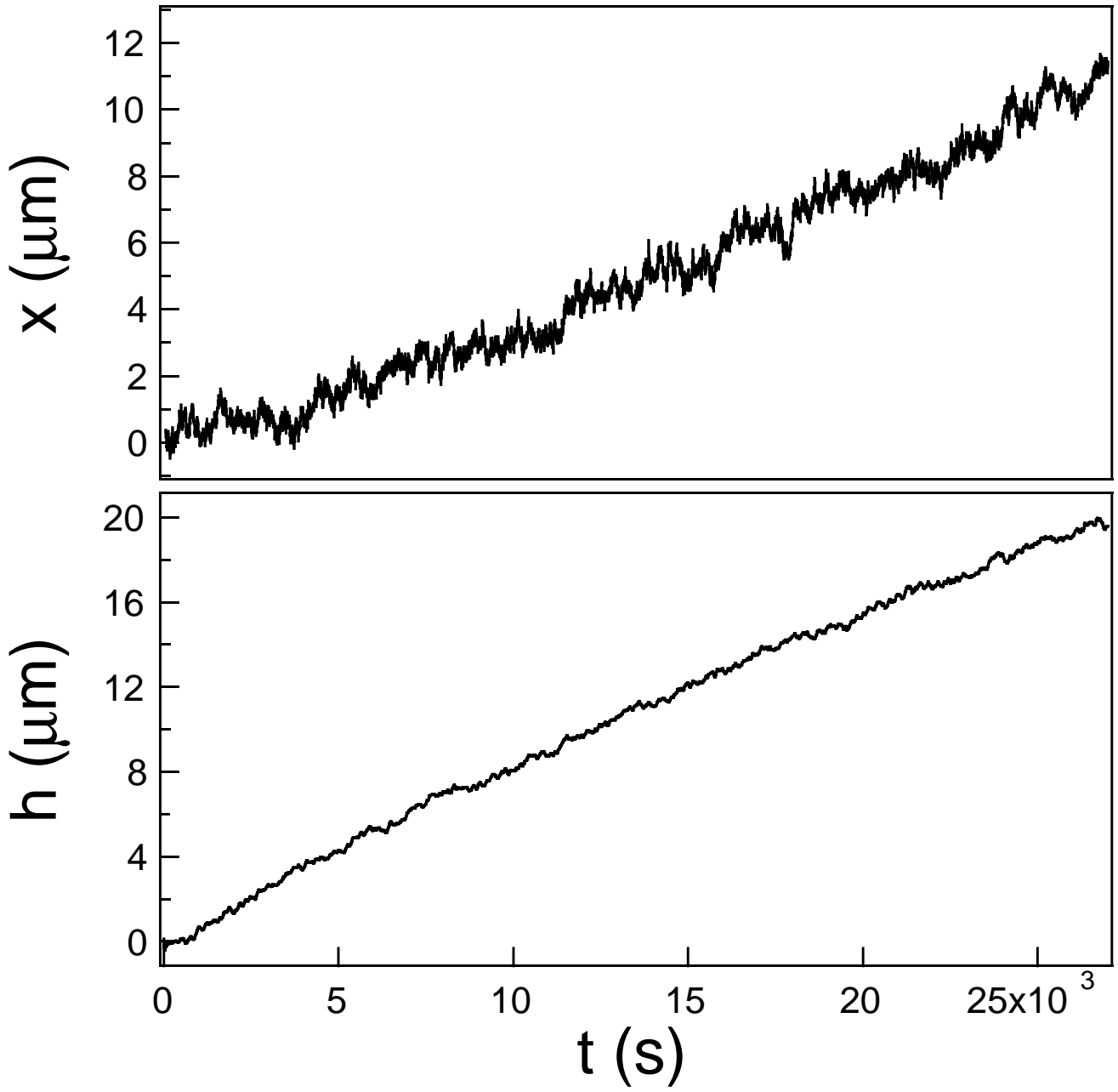


FIG. 11. (Wet friction) Horizontal and vertical positions of the plate x and h as functions of time t when the system is submitted to a static horizontal applied stress $F \simeq F_d$. Creep of about $1\mu\text{m}/\text{h}$ is clearly evident ($k = 189.5\text{N}/\text{m}$, $M = 14.5\text{g}$).